Comparison of Thermal Characteristics of Sensible and Latent Heat Storage Materials Encapsulated in Different Capsule Configurations

Muthukumar Palanisamy and Hakeem Niyas

Abstract This paper presents the thermal modeling and performance comparison of sensible and latent heat based thermal energy storage (TES) systems using concrete and phase change materials (PCMs) encapsulated in containers of different geometrical configurations. The sensible heat storage (SHS) and latent heat storage (LHS) module considered here is a capsule containing concrete or sodium nitrate which exchanges heat with the source material. SHS capsule is modeled using the energy conservation equation. Effective heat capacity method is employed to account the latent heat of the PCM. Boussinesq approximation and Darcy law's source term are added in the momentum equation to incorporate the natural convection of molten PCM and nullify the velocities of solid PCM. The equations of the 2D axisymmetric model are solved using COMSOL Multiphysics. Charging time of capsules in four different configurations viz., spherical, cylindrical ($H = D$, $H = 4D$) and novel cylindrical configurations are compared. The thermal characteristics are compared using isothermal contour plots and temperature–time curves.

Keywords Encapsulation · Performance prediction · Solar thermal · Energy storage

1 Introduction

Several countries ramped up their investments on renewable energy based electricity generation to combat the harmful environmental outcomes from power plants running on fossil fuels. Indeed the availability of fossil fuels is also a big question after few decades. Concentrated solar power (CSP) is one of the promising large-scale power generation technologies among the renewables which is being widely commercialized now. The major problem that CSP plants face is the

M. Palanisamy (✉) · H. Niyas
Department of Mechanical Engineering, Indian Institute of Technology Guwahati, Guwahati, Assam, India
e-mail: pmkumar@iitg.ernet.in; pmkumariitg@gmail.com

L. Chandra and A. Dixit (eds.), *Concentrated Solar Thermal Energy Technologies*, Springer Proceedings in Energy, https://doi.org/10.1007/978-981-10-4576-9_2

intermittent solar radiation which limits the capacity and reliability of the plant. To alleviate this, integration of thermal energy storage (TES) systems to the CSP plants is essential [1]. Till date, two TES technologies were implemented commercially, viz., molten salt systems for parabolic trough or solar tower CSP plants and steam accumulators for direct steam generation CSP plants [2]. The major disadvantage of steam accumulators is the decrease in pressure during the discharging of steam. Incorporating a flash evaporator or an encapsulated heat storage capsule is preferred to avoid or reduce the pressure drop. Due to entropy generation by mixing in the flash evaporator system, encapsulated capsule is beneficial in steam accumulators [3]. Thermal energy can be stored in the form of sensible heat, latent heat and thermochemical heat. Sensible and latent heat storage devices are viable options for usage in steam accumulators in the form of encapsulated capsules. SHS devices store the sensible heat of the material during the rise in temperature. LHS devices store the latent heat of phase change material (PCM) at near constant melting temperature. But thermal resistance during charging/discharging of certain SHS material like concrete and PCM is high because of its low thermal conductivity. Several techniques were analyzed by researchers to increase the performance of the storage systems [4–6]. A detailed review of performance improvement techniques for was reported in the literature [7]. Encapsulating storage materials inside capsule increases the specific surface area. Also, direct contact of heat transfer fluid with the capsule increases the heat transfer coefficient [8]. Spherical and cylindrical capsules filled with PCM were tested for storage characteristics in a constant temperature bath at lab scale and a steam accumulator at industrial scale [9–13]. It is understood from the literature survey that no work was reported comparing the performance characteristics of different configurations of encapsulated capsules. In the present work, a numerical model is developed for evaluating the performances of different configurations of encapsulated capsules. Concrete and sodium nitrate packed in four different configurations, viz., spherical, cylindrical ($H = D$, $H = 4D$), and novel cylindrical models are compared.

2 Model Description

Figure 1 shows a view of the 2D axisymmetric encapsulated capsule containing concrete or sodium nitrate. The capsules are designed for a heat storage capacity of 320 kJ each. Melting point, latent heat, and thermal conductivity are the major parameters which are having a great influence in the design of any LHS systems. Similarly, specific heat and thermal conductivity of the storage material decides the charging time of SHS systems. The dimensions of the capsules are given in Table 1. Encapsulating material should withstand the high pressures (60–80 bar) that exists inside the pressure vessel. SS304 is selected as the encapsulating material for the present analysis. The thermophysical properties of concrete, sodium nitrate and SS304 are given in Table 2. Three physical processes are to be simulated to study the thermal storage behavior of encapsulated LHS capsules, i.e. conduction,

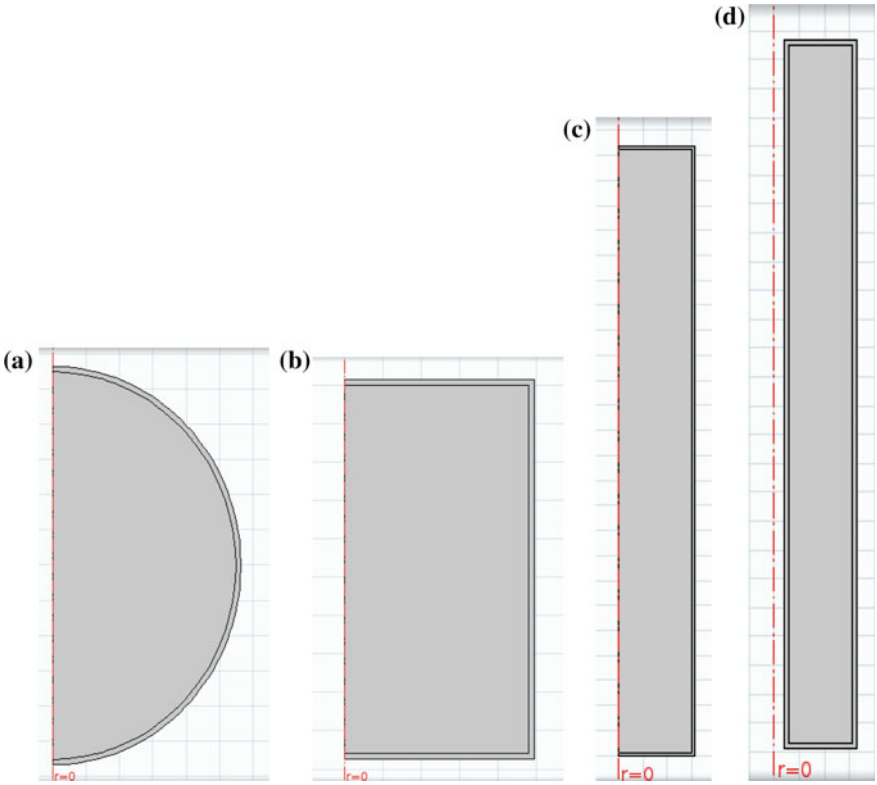

Fig. 1 2D axisymmetric view of capsules **a** spherical **b** cylindrical, $H = D$ **c** cylindrical, $H = 4D$ and **d** novel cylindrical

Table 1 Dimensions of capsules

Configuration	Concrete		Sodium nitrate	
	D (mm)	H (mm)	D (mm)	H (mm)
Spherical	223	–	110	–
Cylindrical ($H = D$)	195	195	96	96
Cylindrical ($H = 4D$)	122.5	490	60.5	242
Novel cylindrical	123	490	61	242

convection and phase change. Conduction heat transfer is the only process involved in the charging simulation of SHS capsules. A 2D axisymmetric model is developed in view of the symmetry of flow and heat transfer around the vertical axis. Molten PCM movement within the capsules due to natural convection heat transfer is assumed to be laminar, Newtonian and incompressible. The major problem

Table 2 Thermo-physical properties of sodium nitrate, concrete and SS304

Properties	Sodium nitrate [15–18]	Concrete [19]	SS304 [19]
ρ (kg/m^3)	2130 (solid) 1908 (liquid)	2300	8000
ΔH_F (J/kg)	178,000	–	–
μ (Pa s)	$0.0119–1.53 \times 10^{-5}\ T$	–	–
T_M (°C)	306.8	–	–
C_P (J/kg K)	$444.53 + 2.18\ T$	800	500
α (1/K)	6.6×10^{-4}	1×10^{-5}	1.78×10^{-5}
k (W/m K)	$0.3057 + 4.47 \times 10^{-4}\ T$	1.2	16.2

associated with the modeling of LHS capsule is the inclusion of latent heat necessary to melt/solidify the PCM. This problem is resolved by using the effective heat capacity method, which takes both specific heat and latent heat of the PCM in a single term called effective heat capacity. The discontinuous modified heat capacity is applied in the COMSOL Multiphysics software using a Heaviside function [14]. Boussinesq approximation and Darcy law's source term are added in the momentum equation to include the buoyancy effect and nullify the solid PCM's velocity. The corresponding governing equations for simulating the capsules are given in Eqs. (1)–(7). Initially, the capsules are at 291.8 °C. At any time ($t > 0$), the boundaries are given a temperature of 321.8 °C thereby making a temperature swing of 30 °C

$$C_P = \begin{cases} C_{PS} & \text{for } T < T_S \\ C_{P,\text{EFF}} & \text{for } T_S \le T \le T_L \\ C_{PL} & \text{for } T > T_L \end{cases} \tag{1}$$

$$C_{P,\text{EFF}} = \frac{C_{PS} + C_{PL}}{2} + \frac{\Delta H_F}{2\Delta T_M} \tag{2}$$

$$\nabla . \vec{V} = 0 \tag{3}$$

$$\frac{\partial \vec{V}}{\partial t} + (\vec{V}.\nabla)\vec{V} = \frac{1}{\rho}\left(-\nabla P + \mu \nabla^2 \vec{V} + F + \vec{S}\right) \tag{4}$$

$$\rho C_p \frac{\mathrm{D}T}{\mathrm{D}t} = k\nabla^2 T \tag{5}$$

$$F = \rho \vec{g} \beta (T - T_M) \tag{6}$$

$$\theta = \frac{T - T_S}{T_L - T_S} = \frac{T - T_M + \Delta T_M}{2\Delta T_M} = \begin{cases} 0 & \text{for } T < T_S \\ 0 - 1 & \text{for } T_S \le T \le T_L \\ 1 & \text{for } T > T_L \end{cases} \tag{7}$$

3 Results and Discussions

3.1 Validation

In order to validate the numerical model, the results obtained for the melt fraction of storage bed were compared with the melt fraction reported in the literature [10]. The physical model chosen for the numerical validation, thermophysical properties of the PCM and initial and boundary conditions of the model are taken from literature [10]. It is evident from Fig. 2 that the current numerical results showed good agreement with the results reported in the literature [10].

3.2 Grid Independency Test

Free triangular mesh has been adapted in the numerical model. In order to test the dependency of numerical results on the mesh element size, a simulation is run with the cylindrical capsule of $H = D$. The LHS capsule is initially at 291.8 °C. At any time $t > 0$, the boundary of the capsule is at 321.8 °C. The average temperature of the capsule is compared for different element sizes and it is observed from Fig. 3 that 10,377 elements can be taken for the numerical model. Similarly, grid independency test carried has been carried out for other configurations also. Time step used in the analyses is 0.01 s throughout all the models.

3.3 Temperature Distribution

Figure 4a, b shows the comparison of the average temperature variation of the LHS/SHS capsules of different configurations. During charging, PCM/concrete kept in the capsules is initially in the solid state at 291.8 °C. When a high temperature of

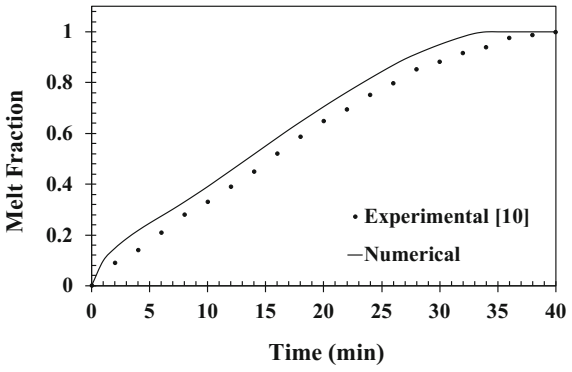

Fig. 2 Validation of the numerical model

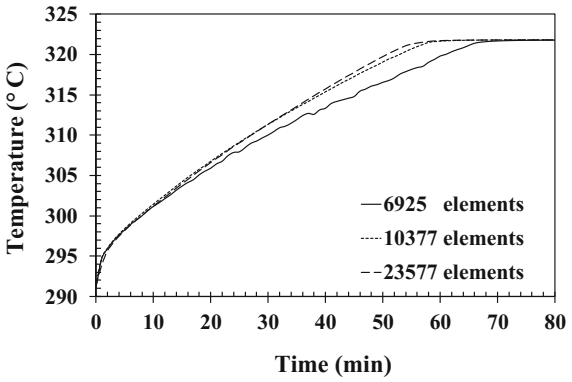

Fig. 3 Grid independency test

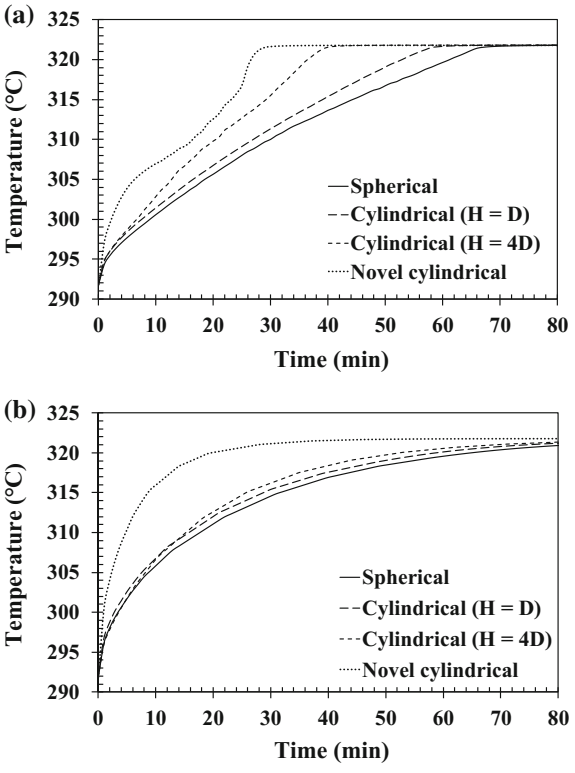

Fig. 4 Temperature variation **a** LHS and **b** SHS capsules

321.8 °C is applied on the boundary of the capsule, heat is transferred from periphery of the capsules and thereby stored in the form of sensible and latent heat. It is inferred from Fig. 4 that the increase in average temperature is faster in cylindrical capsules than the spherical capsule. Also, it can be noted that the cylindrical capsule with a higher aspect ratio reaches the boundary condition in

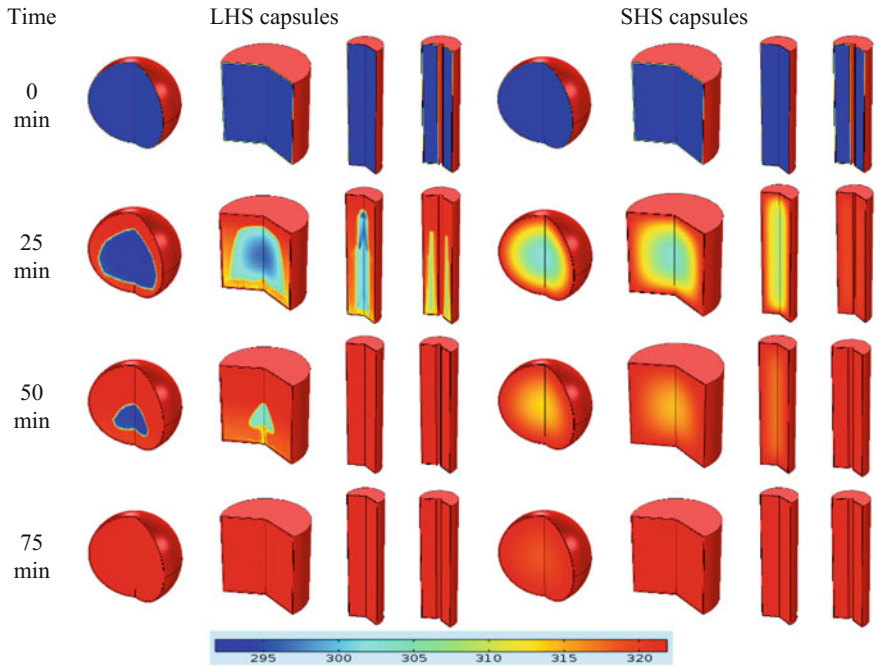

Fig. 5 Temperature variation of LHS and SHS capsules

lesser time. Also, the increase in temperature of novel cylindrical configuration is much faster than all of the configurations. This is due to two reasons, viz., increased heat transfer area and reduced thickness of the capsule. Screenshots of temperature variation of LHS capsules during charging are given in Fig. 5. The effect of natural convection is seen from the asymmetric temperature variation in all the LHS capsules. Similarly, the conduction in the concrete capsules is seen from the symmetric variation of temperature.

3.4 Total Energy Storage Rate

Figure 6a, b show the total energy storage rate of all the LHS/ SHS capsules. For making a comparison between the LHS and SHS capsules of different configurations, the time taken for 95% of total energy stored, i.e., 304 kJ can be taken as the charging time of the capsules. It took about 58, 48, 36, and 26 min to store about 320 kJ in the LHS capsules. Similarly, it took about 69, 62, 57, and 22 min to store about 320 kJ in the SHS capsules.

In the SHS capsules, minor difference in the charging time exists between the spherical, cylindrical ($H = D$), and cylindrical ($H = 4D$) configurations. But there

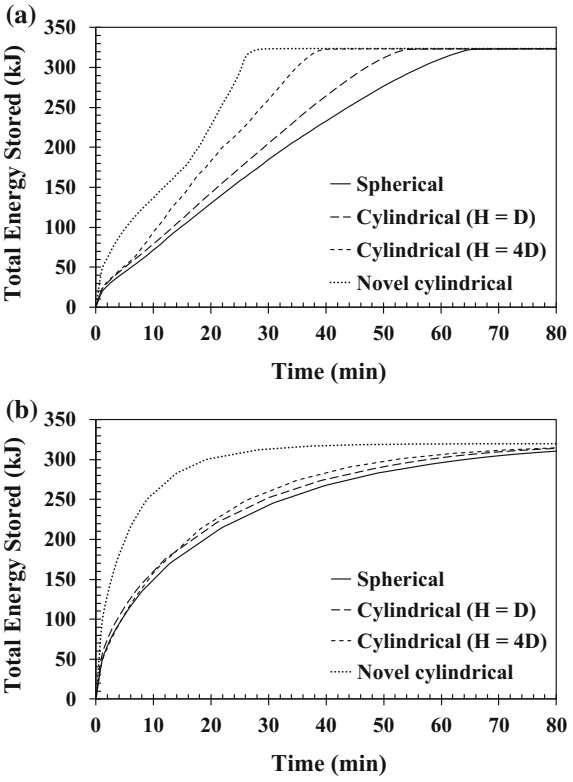

Fig. 6 Total energy storage variation **a** LHS and **b** SHS capsules

exists a huge decrease in the charging time using the novel cylindrical configuration. In the LHS capsules, considerable difference in the charging time exists between the spherical, cylindrical ($H = D$), cylindrical ($H = 4D$), and novel cylindrical configurations. This is due to the presence of natural convection in the capsules during melting. The proposed novel cylindrical configuration yields 61 and 28% lesser charging times for SHS and LHS capsules when compared with the cylindrical capsule ($H = 4D$).

4 Conclusions

A thermal model was developed to compare the performance of LHS/SHS capsules of different geometrical configurations. Numerical results shown that for the same mass of storage material, cylindrical configuration yields lesser charging time than the spherical configuration. This is due to the fact that the distance between the center and periphery of the capsule is more in spherical capsule than that of cylindrical capsule. In the cylindrical models, configuration with a higher aspect

ratio takes lesser time for charging. The time taken for charging of LHS capsule in spherical, cylindrical ($H = D$, $H = 4D$) and novel cylindrical configurations are 58, 48, 36, and 26 min, respectively. Similarly, the time taken for charging of SHS capsule in spherical, cylindrical ($H = D$, $H = 4D$), and novel cylindrical configurations are 69, 62, 57 and 22 min, respectively. The proposed novel cylindrical configuration saves 61 and 28% charging times for SHS and LHS capsules when compared with the cylindrical capsule ($H = 4D$). The results of the current study will be useful in the design and optimization of storage modules which are having wide usage in solar thermal power plants, clean transportation systems, thermal conditioning for buildings, etc.

Acknowledgements The authors sincerely thank the Department of Science and Technology (DST), Government of India, for the financial support (Project No: DST/TM/SERI/2K10/53(G)).

References

1. S.H. Madaeni, R. Sioshansi, P. Denholm, Capacity value of concentrating solar power plants. National Renewable Energy Laboratory Technical Report, NREL/TP-6A20-51253 (2011)
2. C. Prieto, A. Jove, F. Ruiz et al., in *Commercial Thermal Storage. Molten Salts vs. Steam Accumulators*. Proceedings, SolarPACES. http://www.solarpaces2012.org (2012)
3. W.D. Steinmann, M. Eck, Buffer storage for direct steam generation. Sol. Energy **80**, 1277–1282 (2006)
4. I.T. Barney, S. Ganguli, A.K. Roy et al., Improved thermal response in encapsulated phase change materials by nanotube attachment on encapsulating solid. J. Nanotechnol. Eng. Med. **3**, 6–0310051 (2012)
5. A. Sari, A. Karaipekli, Thermal conductivity and latent heat thermal energy storage characteristics of paraffin/expanded graphite composite as phase change material. Appl. Therm. Eng. **27**, 1271–1277 (2007)
6. L.C. Chow, J.K. Zhong, J.E. Beam, Thermal conductivity enhancement for phase change storage media. Int. Commun. Heat Mass Transfer **23**(1), 91–100 (1996)
7. L. Liu, W. Saman, F. Bruno, Review on storage materials and thermal performance enhancement techniques for high temperature phase change thermal storage systems. Renew. Sustain. Energy Rev **16**, 2118–2132 (2012)
8. A. Mathur, R. Kasetty, J. Oxley et al., Using encapsulated phase change salts for concentrated solar power plant. Energy Procedia **49**, 908–915 (2014)
9. C.W. Chan, F.L. Tan, Solidification inside a sphere—an experimental study. Int. Commun. Heat Mass Transfer **33**, 335–341 (2006)
10. E. Assis, L. Katsman, G. Ziskind et al., Numerical and experimental study of melting in a spherical shell. Int. J. Heat Mass Transfer **50**, 1790–1804 (2007)
11. A.R. Archibold, M.M. Rahman, D.Y. Goswami et al., Analysis of heat transfer and fluid flow during melting inside a spherical container for thermal energy storage. Appl. Therm. Eng. **64**, 396–407 (2014)
12. N. Himeno, K. Hijikata, A. Sekikawa, Latent heat thermal energy storage of a binary mixture-flow and heat transfer characteristics in a horizontal cylinder. Int. J. Heat Mass Transfer **31**(2), 359–366 (1988)
13. W.D. Steinmann, R. Tamme, Latent heat storage for solar steam systems. J. Sol. Energy Eng. **130**, 5–0110041 (2008)
14. COMSOL Inc., http://www.comsol.com/

15. T. Bauer, D. Laing, R. Tamme, Characterization of sodium nitrate as phase change material. Int. J. Thermphys. **33**, 91–104 (2012)
16. G.J. Janz, C.B. Allen, N.P. Bansal et al., Physical Properties Data Compilations Relevant to Energy Storage. II. Molten Salts: Data on Single and Multi-component Salt Systems. NSRDS-NBS-61. http://www.nist.gov/data/nsrds/NSRDS-NBS61-II.pdf (1979)
17. C.W. Lan, S. Kou, Effects of rotation on heat transfer, fluid flow and interfaces in normal gravity floating-zone crystal growth. J. Cryst. Growth **114**, 517–535 (1991)
18. L.R. White, H.T. Davis, Thermal conductivity of molten alkali nitrates. J. Chem. Phys. **47**, 5433–5439 (1967)
19. AZo Network UK Ltd., http://www.azom.com/

http://www.springer.com/978-981-10-4575-2

Concentrated Solar Thermal Energy Technologies
Recent Trends and Applications
Chandra, L.; Dixit, A. (Eds.)
2018, XV, 276 p. 137 illus., Hardcover
ISBN: 978-981-10-4575-2